How robust are observed and simulated precipitation responses to tropical ocean warming?

Viju O. John,[1] Richard P. Allan,[2] and Brian J. Soden[3]

Received 22 March 2009; revised 6 May 2009; accepted 27 May 2009; published 17 July 2009.

[1] Robust responses and links between the tropical energy and water cycles are investigated using multiple datasets and climate models over the period 1979–2006. Atmospheric moisture and net radiative cooling provide powerful constraints upon future changes in precipitation. While moisture amount is robustly linked with surface temperature, the response of atmospheric net radiative cooling, derived from satellite data, is less coherent. Precipitation trends and relationships with surface temperature are highly sensitive to the data product and the time-period considered. Data from the Special Sensor Microwave Imager (SSM/I) produces the strongest trends in precipitation and response to warming of all the datasets considered. The tendency for moist regions to become wetter while dry regions become drier in response to warming is captured by both observations and models. **Citation:** John, V. O., R. P. Allan, and B. J. Soden (2009), How robust are observed and simulated precipitation responses to tropical ocean warming?, *Geophys. Res. Lett.*, *36*, L14702, doi:10.1029/2009GL038276.

1. Introduction

[2] An important consequence of global warming is a changing water cycle, with potentially adverse impacts on societies and the ecosystems upon which they depend. Climate models project global average precipitation (P) to rise with temperature, with an increased intensity of rainfall yet a greater proportion of the sub-tropics affected by drought conditions [*Meehl et al.*, 2007].

[3] While regional predictions of precipitation are uncertain [*Meehl et al.*, 2007], the large-scale tendencies of the hydrological cycle can be understood in terms of theoretical considerations. Models and observations agree that column integrated water vapor (W) rises with surface temperature (T_s) in accordance with the Clausius Clapeyron equation (C-C), approximately 7% K^{-1} [*Held and Soden*, 2006]. Since moisture convergence is required to feed large-scale and convective precipitation, there is a physical basis for expecting comparable increases in the intensity of rainfall events [*Trenberth et al.*, 2003], backed up by models and limited observational evidence [*Allan and Soden*, 2008; *Lenderink and Van Meijgaard*, 2008].

[4] Global precipitation, however, is not regulated by the availability of moisture but by atmospheric energy balance. Enhanced net radiative cooling of the atmosphere in a warming climate requires an increase in latent heating from precipitation [*Allen and Ingram*, 2002; *Held and Soden*, 2006], assuming small changes in sensible heat flux [*Stephens and Ellis*, 2008]. If the heaviest precipitation increases at a greater rate than the mean, this implies a reduced frequency and/or intensity away from such regimes; this is consistent with emerging observational and modeling evidence of moist tropical regions becoming wetter at the expense of dry regions [*Allan and Soden*, 2007; *Chou et al.*, 2007].

[5] Observational studies have suggested rises in P and Evaporation (E) at the rate expected from C-C [*Wentz et al.*, 2007], substantially larger than predicted by the models [*Held and Soden*, 2006]. The muted response of P and E in the models, relative to the C-C rate, is readily explained by atmospheric net radiative cooling [*Lambert and Webb*, 2008] or by small yet systematic changes in surface wind, humidity and temperature [*Richter and Xie*, 2008]. Aside from radiative perturbations involving aerosol [e.g., *Wild et al.*, 2008], it is difficult to explain apparently larger changes in P over recent decades, raising the question of whether the observed responses are statistical artifacts [*Liepert and Previdi*, 2009] or a consequence of poorly constrained assumptions relating to calibration and construction of long-term records of P or E [*Adler et al.*, 2008; *Stephens and Ellis*, 2008].

[6] In this study we analyse multiple satellite derived estimates of water and energy cycle variables, using data from the Global Precipitation Climatology Project version 2 (GPCP) [*Adler et al.*, 2008], the Special Sensor Microwave Imager, version 6 (SSM/I) [*Hilburn and Wentz*, 2008], the Scanning Multi-channel Microwave Radiometer (SMMR) [*Prabhakara et al.*, 1982], the Tropical Rainfall Measurement Mission (TRMM) [*Robertson et al.*, 2003], and radiation budget data from the Surface Radiation Budget project (SRB) [*Zhang et al.*, 2006] and the Clouds and the Earth's Radiant Energy System version Terra-FM1-MODIS_Edition2D (CERES) [*Wielicki et al.*, 1996]. Also employed were reanalysis data from the National Center for Environmental Prediction (NCEP) [*Kalnay et al.*, 1996] and the European Centre for Medium range Weather Forecasts Interim reanalysis (ERA Interim) based on *Uppala et al.* [2005] and climate model experiments, using observed sea surface temperature forced atmosphere-only (AMIP3) and fully-coupled (CMIP3) configurations [*Meehl et al.*, 2007]. Variability in W, T_s, P, atmospheric longwave radiative cooling rate (Q_{LW}) and shortwave radiative heating rate (Q_{SW}) are analysed over the period 1979–2006, using reanalysis vertical velocity at 500 hPa (ω_{500}) to differentiate

[1]Met Office Hadley Centre, Exeter, UK.
[2]Environmental Systems Science Centre, University of Reading, Reading, UK.
[3]Rosenstiel School for Marine and Atmospheric Science, University of Miami, Miami, Florida, USA.

0094-8276/09/2009GL038276$05.00

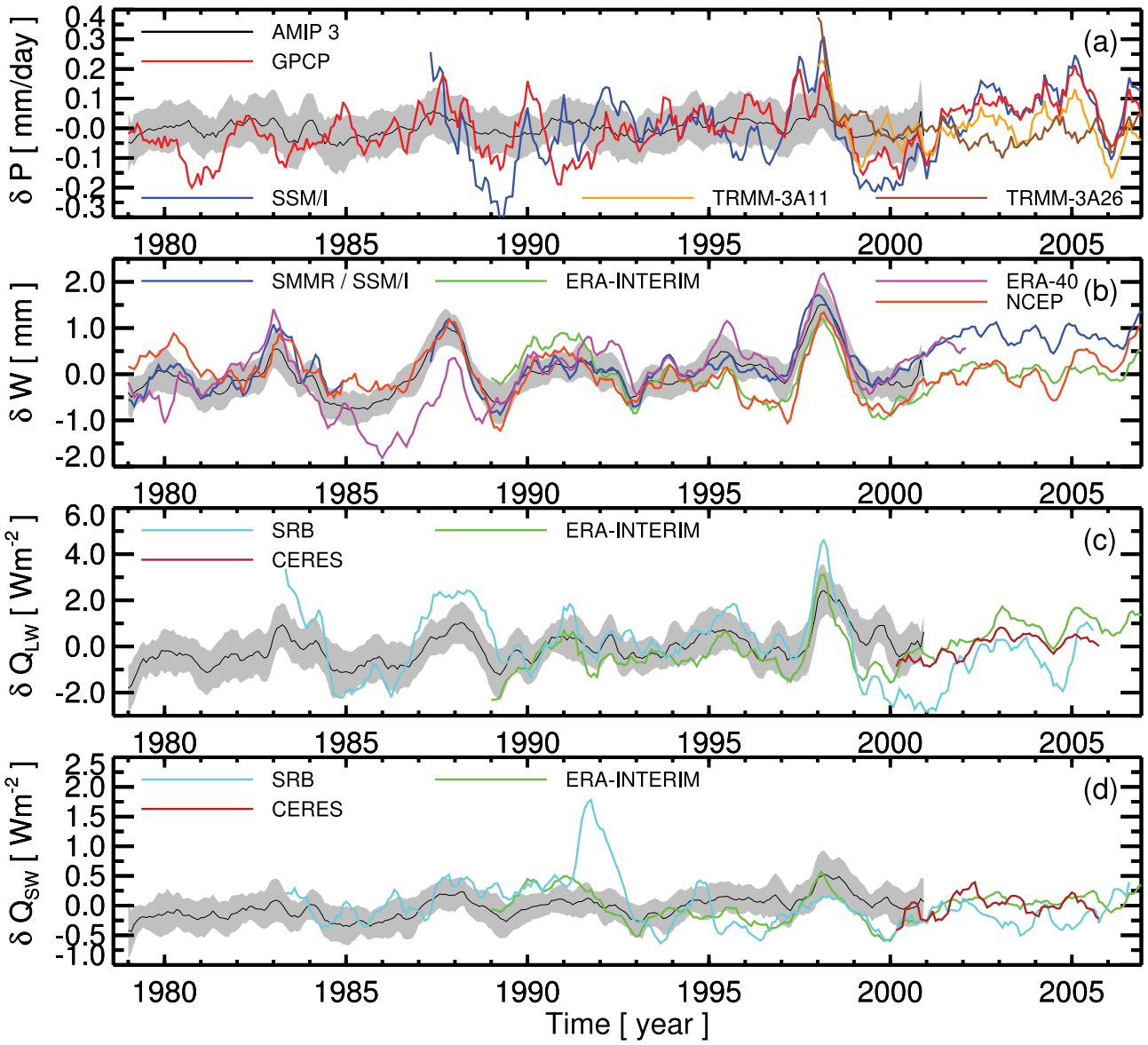

Figure 1. Deseasonalized, area weighted tropical ocean anomalies in (a) precipitation rate (P), (b) total column water vapor (W), (c) longwave radiative cooling rate (Q_{LW}), and (d) shortwave radiative heating rate (Q_{SW}) for observations, reanalyses and AMIP3 models. The shaded region denotes ± one standard deviation of AMIP3 inter-model variability.

ascending and descending regions [*Allan and Soden*, 2007]. Specifically, we discuss whether discrepancies relate to the constraining variables, W and net radiative cooling, or are sensitive to the time-period and satellite instrument employed. Finally, do robust responses of the hydrological cycle emerge from recent decades that are pertinent to the future projections of climate?

2. Variability in Energy and Water Cycles

[7] Components of the hydrological and energy cycles from observations, reanalyses and current climate models are displayed in Figure 1 for the tropical oceans (±30° latitude) over the period 1979–2006. We select this domain to maximize a) the coverage and accuracy of the observational datasets and b) the substantial interannual variability of the variables relating to El Niño. This is a limitation in linking the energy and water cycles, since we are not accounting for variations in energy export to the extra tropics. Nevertheless, *Soden* [2000] found that results are not very sensitive to selecting a more extensive domain. Multi-model ensemble mean (black line) and ±1 standard deviation (shaded area) are computed each month using the AMIP3 models listed in Table 1 for the period 1979–2000. Coloured lines show different observationally-based data sets.

[8] Precipitation anomalies from GPCP, SSM/I, and TRMM passive microwave (3A11) and active radar (3A26) retrievals, are compared with the models in Figure 1a. Increased rainfall is apparent during the warm El Niño of 1997/98. However, there are large discrepancies between the different data sets and the model ensemble mean,

Table 1. Correlation (r) and Slope (a) of Different Components of Hydrologic and Energy Cycles to Changes in Sea Surface Temperature[a]

		P		W		Q_{LW}		Q_{SW}	
Model	Period	r	a	r	a	r	a	r	a
BCC_CM_1	1980–2000	0.50	0.16	-	-	-	-	-	-
CNRM_CM3	1980–2000	0.22	0.09	0.88	3.47	0.58	3.66	0.49	0.79
GISS_MODEL_E_R	1980–2000	0.72	0.22	0.97	3.54	-	-	-	-
IAP_FGOALS1_0_G	1980–2000	0.19	0.06	0.93	3.05	-	-	0.86	0.83
INMCM3_0	1980–2000	0.57	0.19	0.91	2.56	0.61	3.65	0.75	0.83
MIROC3_2_HIRES	1980–2000	0.57	0.22	0.91	2.85	0.67	3.45	0.67	1.41
MIROC3_2_MEDRES	1980–2000	0.35	0.11	0.86	2.53	0.66	3.50	0.32	0.68
MPI_ECHAM5	1980–2000	0.22	0.09	0.91	3.88	0.75	4.54	0.77	1.27
MRI_CGCM2_3_2A	1980–2000	0.15	0.05	0.88	3.00	0.45	2.62	0.37	0.39
NCAR_CCSM3_0	1980–2000	0.52	0.16	0.94	3.68	0.72	5.18	0.80	1.18
NCAR_PCM1	1980–2000	0.55	0.16	0.89	3.66	-	-	-	-
UKMO_HADGEM1	1980–2000	0.46	0.14	-	-	-	-	0.76	1.89
Model Ensemble	1980–2000	0.72	0.14	0.98	3.20	0.75	3.80	0.80	1.01
SSM/I	1987–2006	0.67	0.54	0.95	3.39	-	-	-	-
SRB	1983–2006	-	-	-	-	0.46	4.21	0.10	0.18
ERA-INTERIM	1989–2006	−0.40	−0.28	0.57	1.77	0.84	5.49	0.56	0.95

[a] a is the slope of the linear regression and r is the correlation coefficient. a has units of mm/day/K for P, mm/K for W, W m^2/K for Q_{LW} and Q_{SW}, and r has no units. All available models except GISS are used to calculate model ensemble mean for each variable.

highlighting our limited confidence in recent changes in mean precipitation.

[9] Can observed changes in the energy and water cycles help improve our understanding of present day variability in P? Figure 1b presents tropical-mean anomalies in W derived from SMMR (1979–84) and SSM/I for July 1987–2006. Excellent agreement between observations and AMIP simulations are consistent with previous studies [*Soden*, 2000], both showing increased atmospheric water content during warm El Niño events. This suggests that changes in the moisture available for condensation and precipitation is well understood and cannot offer an explanation for precipitation discrepancies between the models and observations. We also show W from reanalysis data: NCEP and ERA Interim show realistic variability but fail to capture the observed increasing trend where as ERA-40 (using the 24-hour forecast products) shows anomalous variability. This, as well as reductions in P for ERA Interim (see Table 1), suggest current reanalysis products remain unable to represent trends in the water cycle [e.g., *Bengtsson et al.*, 2004].

[10] Do observed changes in the atmospheric radiation balance provide an observational constraint upon changes in precipitation? Figure 1c shows Q_{LW} anomalies from SRB, CERES, and ERA-Interim. There is some agreement between datasets, for example more cooling during El Niño events. However, the observationally-based estimates themselves do not show a consistent picture and thus are not sufficient to constrain the modeled values. Similarly, Q_{SW} anomalies from the same data sources show substantial discrepancies (Figure 1d). The discrepancy in 1991/92 shows the effect of aerosols from the Pinatubo volcanic eruption which were approximated in SRB but were not included in ERA Interim and AMIP models (The GISS model did include Pinatubo aerosols but this model was excluded from the ensemble mean). While changes in cloud strongly affect surface and top of atmosphere radiation, their influence on atmospheric net radiative cooling is thought to be a secondary effect [*Stephens and Ellis*, 2008; *Lambert and Webb*, 2008] and variability in Q_{LW} and Q_{SW} are dominated by clear-sky changes which are dependent

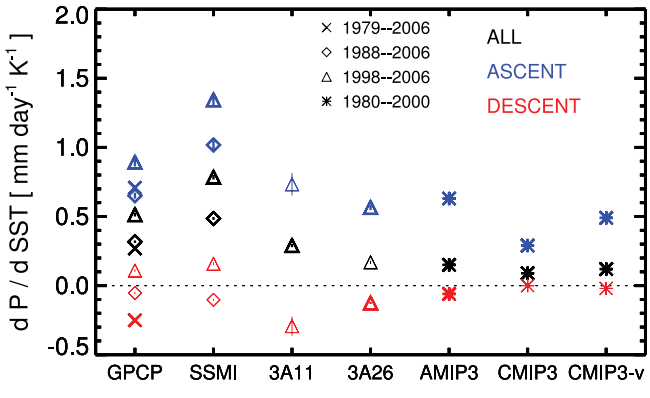

Figure 2. Sensitivities of observational and model simulated precipitation to T_s. Symbols represent time periods. Colours differentiate ascending or descending (or both) regimes. Bold symbols show significant correlations. Vertical bars represent one sigma uncertainty of sensitivity.

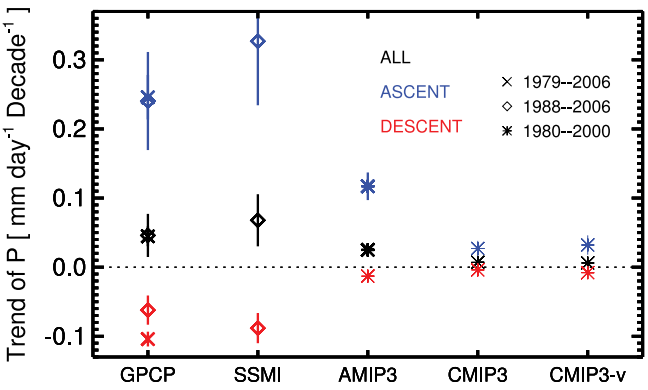

Figure 3. Same as Figure 2 but for trends in P.

upon reanalysis datasets, themselves prone to erroneous variability (Figure 1b).

3. Sensitivity to Sea Surface Temperature

[11] Correlations and sensitivities (which is the slope of linear regression) of P, W, Q_{LW}, and Q_{SW} to changes in T_S are given in Table 1 for the models and the data products. All models show good correlation between changes in P and T_s but the sensitivity is at least 2 times smaller than SSM/I. ERA Interim data show a negative correlation and sensitivity, at odds with other datasets considered.

[12] Inter-model variability for W varies less and the values are in good agreement with observations. This confirms that the discrepancy in precipitation cannot be explained by the models' poor simulations of water vapor. ERA Interim shows less sensitivity compared to other observations and models.

[13] All datasets and models show a positive relationship between Q_{LW} and T_s, ranging from 2.6–5.5 $Wm^{-2}K^{-1}$. The positive relationship is an expected consequence of atmospheric warming with unchanging relative humidity, but is lower than the clear-sky value [*Allan*, 2009]. An additional expected consequence of atmospheric moistening is enhanced Q_{SW} which rises by around 1.0 $Wm^{-2}K^{-1}$ in most models and ERA Interim although the slope is stronger for HadGEM1, weaker for the MRI CGCM model and the SRB data (the Pinatubo period 1991–92 was removed from the SRB Q_{SW} time series in these calculations).

[14] While there is broad agreement in the responses of Q_{SW} and Q_{LW} to warming, there is little relationship between the net radiative cooling ($Q_{LW} - Q_{SW}$) sensitivity to warming and dP/dT_s in the models suggesting that analysing the tropical ocean radiative energy balance does not constraint changes in P. We may only state that rises in P are consistent with rises in net radiative cooling with warming in all datasets apart from ERA Interim, which is not subject to balance in the energy and water budgets.

4. Data Set and Time Period Dependence

[15] In this section we investigate whether the precipitation discrepancy can be explained by inadequacies of the observations. Figure 2 shows response of P to changes in T_S for observations and model ensembles (CMIP3 values are taken from *Allan* [2009]). Here the analysis is done for different dynamic regimes (ascending or descending) based on the NCEP reanalysis ω_{500} and are shown in different colours. Symbols plotted in bold show significant correlation above the 95% confidence level.

[16] In general, sensitivity to T_s is not robust between data sets. The dependence on satellite instrument and time periods is substantial. For the ascent region, the SSM/I sensitivity shows a range of 0.4 mm/day/K, while for the 1998–2006 time period, TRMM radar retrievals display a sensitivity less than half that of SSM/I (Figure 2). Sensitivity in the AMIP3 model ensemble is similar to the TRMM data, although it samples a different time period. CMIP3 models (non volcanic) show less sensitivity compared to AMIP3 models. This is likely to represent the effect of El Niño on the calculated sensitivity; these are essentially removed from the CMIP3 ensemble since they occur at different times in the fully coupled models. Sensitivity in P is also affected by volcanic eruptions as shown by the difference between CMIP3 and the model ensemble with volcanic forcing included (CMIP3-v). The robust response in all datasets is an increase in ascent region P with warming and neutral or declining P with warming in descent regions.

[17] Figure 3 shows trends for different observations and model ensembles. We do not show TRMM products here due to their shorter time periods. SSM/I shows the largest trend. Both models and observations show increasing trends in ascending areas and decreasing trend in descending areas. This is physically consistent with the arguments presented in Sec. 1. However, the negative trends of around −10% per decade in descent regions are substantial and require further scrutiny and may relate to errors in the NCEP ω_{500} fields. For example, should ω_{500} fields become more realistic with time, reduced misclassification of wet pixels in the descent region will produce an artificial drying trend (W. Ingram, personal communication, 2009). Indeed, applying more current ERA Interim reanalysis ω_{500} reduces the drying trends magnitude by around 0.04 mm/day/decade (not shown).

5. Summary and Conclusions

[18] Multiple observations and model realisations were used to investigate links between the hydrological and energy cycles of the tropical oceans and the robust nature of trends and responses to warming. Discrepancies between variability in precipitation (P) are substantial, not only between models and observations but between the observational estimates themselves. The SSM/I dataset exhibits the strongest trends and sensitivity of P to surface warming, 1.35 mm/day/K for 1998–2006 for the ascent region, more than double the AMIP3 model ensemble mean and the TRMM radar retrievals.

[19] Observationally-based changes in water vapor are well captured by models and this provides a robust constraint on changes in ascent region precipitation and in particular the frequency/intensity of heavy rainfall events [*Trenberth et al.*, 2003; *Allan and Soden*, 2008]. However, current reanalyses, including ERA Interim, remain unable to realistically capture trends in water vapor and precipitation. The atmospheric radiative energy balance provides a powerful constraint on future global precipitation changes [*Allen and Ingram*, 2002; *Lambert and Webb*, 2008], but this does not appear to apply to the tropical oceans. Further, observed changes in atmospheric radiative fluxes are highly dependent upon reanalysis products and so are therefore also unrealistic.

[20] All observations and models show increasing P with time and with warming for the ascent region while P declines or remains constant in the descent region, consistent with theoretical considerations [*Stephens and Ellis*, 2008; *Allen and Ingram*, 2002]. The observed magnitude of these changes remains uncertain, requiring improvements in the observing system.

[21] **Acknowledgments.** Thanks to the WCRP and PCMDI for providing the model data. This work was supported by grants from the NASA Energy and Water cycle Study, the NOAA Climate Program Office, the UK National Centre for Earth Observation, the NERC grant NE/C51785X/1, and the U.K. Joint DECC, DEFRA, and MoD Integrated Climate Programme - GA01101, CBC/2B/0417_Annex C5. Datasets were supplied by www.ncdc.noaa.gov, www.ssmi.com, www.ecmwf.int and the NASA

Langley Atmospheric Science Data Center. We also thank two anonymous reviewers, D. E. Parker, and S. A. Buehler for their constructive comments.

References

Adler, R. F., G. Gu, J.-J. Wang, G. J. Huffman, S. Curtis, and D. Bolvin (2008), Relationships between global precipitation and surface temperature on interannual and longer timescales (1979–2006), *J. Geophys. Res.*, *113*, D22104, doi:10.1029/2008JD010536.

Allan, R. P. (2009), Examination of relationships between clear-sky longwave radiation and aspects of the atmospheric hydrological cycle in climate models, reanalyses and observations, *J. Clim.*, *22*(11), 3127–3145, doi:10.1175/2008JCLI2616.1.

Allan, R. P., and B. J. Soden (2007), Large discrepancy between observed and simulated precipitation trends in the ascending and descending branches of the tropical circulation, *Geophys. Res. Lett.*, *34*, L18705, doi:10.1029/2007GL031460.

Allan, R. P., and B. J. Soden (2008), Atmospheric warming and the amplification of precipitation extremes, *Science*, *321*, 1481–1484, doi:10.1126/science.1160787.

Allen, M. R., and W. J. Ingram (2002), Constraints on future changes in climate and hydrologic cycle, *Nature*, *419*, 224–232.

Bengtsson, L., S. Hagemann, and K. I. Hodges (2004), Can climate trends be calculated from reanalysis data?, *J. Geophys. Res.*, *109*, D11111, doi:10.1029/2004JD004536.

Chou, C., J.-Y. Tu, and P.-H. Tan (2007), Asymmetry of tropical precipitation change under global warming, *Geophys. Res. Lett.*, *34*, L17708, doi:10.1029/2007GL030327.

Held, I. M., and B. J. Soden (2006), Robust responses of the hydrological cycle to global warming, *J. Clim.*, *19*, 5686–5699.

Hilburn, K. A., and F. J. Wentz (2008), Intercalibrated passive microwave rain products from the unified microwave ocean retrieval algorithm (UMORA), *J. Appl. Meteorol. Climatol.*, *47*, 778–794.

Kalnay, E., et al. (1996), The NCEP/NCAR 40-year reanalysis project, *Bull. Am. Meteorol. Soc.*, *77*, 437–471.

Lambert, F. H., and M. J. Webb (2008), Dependency of global mean precipitation on surface temperature, *Geophys. Res. Lett.*, *35*, L16706, doi:10.1029/2008GL034838.

Lenderink, G., and E. Van Meijgaard (2008), Increase in hourly precipitation extremes beyond expectations from temperature changes, *Nat. Geosci.*, *1*, 511–514, doi:10.1038/ngeo262.

Liepert, B. G., and M. Previdi (2009), Do models and observations disagree on the rainfall response to global warming?, *J. Clim.*, *22*(11), 3156–3166, doi:10.1175/2008JCLI2472.1.

Meehl, G., et al. (2007), Global climate projections, in *Climate Change 2007: The Physical Science Basis. Contribution of Working Group I to the Fourth Assessment Report of the Intergovernmental Panel on Climate Change*, edited by S. Solomon et al., pp. 747–845, Cambridge Univ. Press, Cambridge. U. K.

Prabhakara, C., H. D. Chang, and T. C. Chang (1982), Remote sensing of precipitable water over the oceans from nimbus 7 microwave measurements, *J. Appl. Meteorol.*, *21*, 59–68.

Richter, I., and S.-P. Xie (2008), Muted precipitation increase in global warming simulations: A surface evaporation perspective, *J. Geophys. Res.*, *113*, D24118, doi:10.1029/2008JD010561.

Robertson, F. R., D. E. Fitzjarrald, and C. D. Kummerow (2003), Effects of uncertainty in TRMM precipitation radar path integrated attenuation on interannual variations of tropical oceanic rainfall, *Geophys. Res. Lett.*, *30*(4), 1180, doi:10.1029/2002GL016416.

Soden, B. J. (2000), The sensitivity of the tropical hydrological cycle to ENSO, *J. Clim.*, *13*, 538–549.

Stephens, G. L., and T. Ellis (2008), Controls of global-mean precipitation increases in global warming GCM experiments, *J. Clim.*, *21*, 6141–6155.

Trenberth, K. E., A. Dai, R. M. Rasmussen, and D. B. Parsons (2003), The changing character of precipitation, *Bull. Am. Meteorol. Soc.*, *84*, 1205–1217.

Uppala, S. M., et al. (2005), The ERA-40 re-analysis, *Q. J. R. Meteorol. Soc.*, *131*, 2961–3012.

Wentz, F. J., L. Ricciardulli, K. Hilburn, and C. Mears (2007), How much more rain will global warming bring?, *Science*, *317*, 233–235.

Wielicki, B. A., B. R. Barkstrom, E. F. Harrison, R. B. Lee, G. L. Smith, and J. E. Cooper (1996), Clouds and the Earth's radiant energy system (CERES): An Earth observing system experiment, *Bull. Am. Meteorol. Soc.*, *77*, 853–868.

Wild, M., J. Grieser, and C. Schär (2008), Combined surface solar brightening and increasing greenhouse effect support recent intensification of the global land-based hydrological cycle, *Geophys. Res. Lett.*, *35*, L17706, doi:10.1029/2008GL034842.

Zhang, Y., W. B. Rossow, and P. W. Stackhouse Jr. (2006), Comparison of different global information sources used in surface radiative flux calculation: Radiative properties of the near-surface atmosphere, *J. Geophys. Res.*, *111*, D13106, doi:10.1029/2005JD006873.

R. P. Allan, Environmental Systems Science Centre, University of Reading, Earley Gate, Reading RG6 6AL, UK.

V. O. John, Met Office Hadley Centre, FitzRoy Road, Exeter EX1 3PB, UK. (viju.john@metoffice.gov.uk)

B. J. Soden, Rosenstiel School for Marine and Atmospheric Science, University of Miami, 4600 Rickenbacker Causeway, Miami, FL 33149, USA.